

Oxygen issue in Core Collapse Supernovae.

Abouazza Elmhamdi,

Department of Physics and Astronomy, King Saud University, PO Box 2455, Riyadh
11451, Saudi Arabia
e-mail: elmhamdi@ksu.edu.sa

Received 2011

ABSTRACT

We study the spectroscopic properties of a selected sample of 26 events within Core Collapse Supernovae (CCSNe) family. Special attention is paid to the nebular oxygen forbidden line [O I] 6300,6364Å doublet. We analyze the line flux ratio “ F_{6300}/F_{6364} ”, and infer information about the optical depth evolution, densities, volume-filling factors in the oxygen emitting zones. The line luminosity is measured for the sample events and its evolution is discussed on the basis of the bolometric light curve properties in type II and in type Ib-c SNe. The luminosities are then translated into oxygen abundances using two different methods. The resulting oxygen amounts are combined with the recovered ^{56}Ni masses and compared with theoretical models by means of the “[O/Fe] .vs. M_{ms} ” diagram. Two distinguishable and continuous populations, corresponding to Ib-c and type II SNe, are found. The higher mass nature of the ejecta in type II objects is also imprinted on the [Ca II] 7291,7324Å over [O I] 6300,6364Å luminosity ratios. Our results may be used as input parameters for theoretical models studying the chemical enrichment of galaxies.

Key words: Stars: Supernovae – Core Collapse; Nebular spectra; Yields: Oxygen and Iron

1. Introduction

Recently, interest has increased the interpretation of Core Collapse Supernovae (CCSNe) data, both spectra and photometry (Richardson et al. 2006; Elmhamdi et al. 2006; Taubenberger et al. 2009; Maurer et al. 2010; Elmhamdi et al. 2011). In particular special attention has been devoted to the stripped-envelope events (i.e. type Ib-c hydrogen-deficient SNe). Studying enlarged samples of CCSNe objects, having good quality observations, can be a potential tool for assessing the similarities and the diversities within this SNe family, relating these facts to the physics and possibly to the nature of their progenitors. As an example, Elmhamdi et al. 2006 have presented an investigation of the spectroscopic properties of a selected optical photospheric spectra of CCSNe, discussing how hydrogen manifests its presence within this class. The authors argued for a low mass thin hydrogen layer with very high ejection velocities above the helium shell to be the most likely scenario for

type Ib SNe. Although the primary goal of the the cited work was highlighting the hydrogen traces in CCSNe, an important by-product result concerns the behaviour of oxygen, in particular the O I 7773 Å line. Based on the synthetic spectra fits, for this line it seems that at intermediate photospheric phases, type Ib objects tend to have low optical depths, while some type Ic SNe, e.g. SN Ic 1987M, are found to display the deepest O I 7773 Å profile. SNe of type IIb & II, at similar phases, are found to be the objects with the lowest O I 7773 Å optical depth. At somewhat later epochs, transient type Ib/c objects display deep O I 7773 Å troughs. Matheson et al. (2002) arrived at similar conclusions, indicating the O I 7773 Å line to be stronger in SNe Ic than in SNe Ib.

Interestingly, the deeper and stronger permitted oxygen line O I 7773 Å in photospheric spectra of SNe Ic and Ib/c might imply that they are less diluted by the presence of a helium envelope. We expect indeed the oxygen lines to be more prominent for a “naked” C/O progenitor core. Two further observational aspects tend to reinforce this belief: first, the forbidden lines, especially the [O I] 6300,6364 Å doublet, seem to appear earlier following a SNe sequence “Ic – Ib – IIb – II”. The second indication comes from the fact that this nebular emission line has a velocity width decreasing following the SNe sequence above.

In the present work we explore these points and other issues related to oxygen lines within the CCSNe family, especially at late nebular phases. We analyze a sample of 26 CCSNe events, and quantify the [O I] 6300,6364 Å luminosities and discuss their evolution in time. The [Ca II] 7291,7324 Å over [O I] 6300,6364 Å flux ratio is also shown and discussed as a possible progenitor mass indicator (Fransson & Chevalier 1989). Using the the computed luminosities we discuss two methods to translate these measurements into masses. The estimated oxygen masses are combined then with the measured nickel masses, determined from light curves, and compared with yields from three known theoretical CCSNe models by means of the oxygen-to-iron mass ratio. This is potentially important since our measurements can be directly correlated to the progenitor masses from theoretical models.

Worth noting here is the importance of oxygen and iron estimates, from supernovae explosions, in the chemical enrichment and evolution of galaxies. In particular, the oxygen abundance is crucial in metal-poor stars, and is a key issue in modeling the early phases of the chemical galaxy evolution and as well in constraining the age of globular clusters (VandenBerg et al. 2000; Melendez et al. 2001). Oxygen is indeed considered as a major tracer of chemical evolution, since it is one of primary elements ejected by CCSNe (i.e. resulting from massive stars). For example the oxygen-to-iron ratio, when $[O/Fe] > 0$ such as in the halo of our Galaxy, is an indicator of early chemical enrichment by massive stars.

The paper is organized as follows. In Section 2, we describe the sample and we highlight the main spectroscopic characteristics and differences within the CCSNe family. Some constructed quasi-bolometric light curves are also shown and

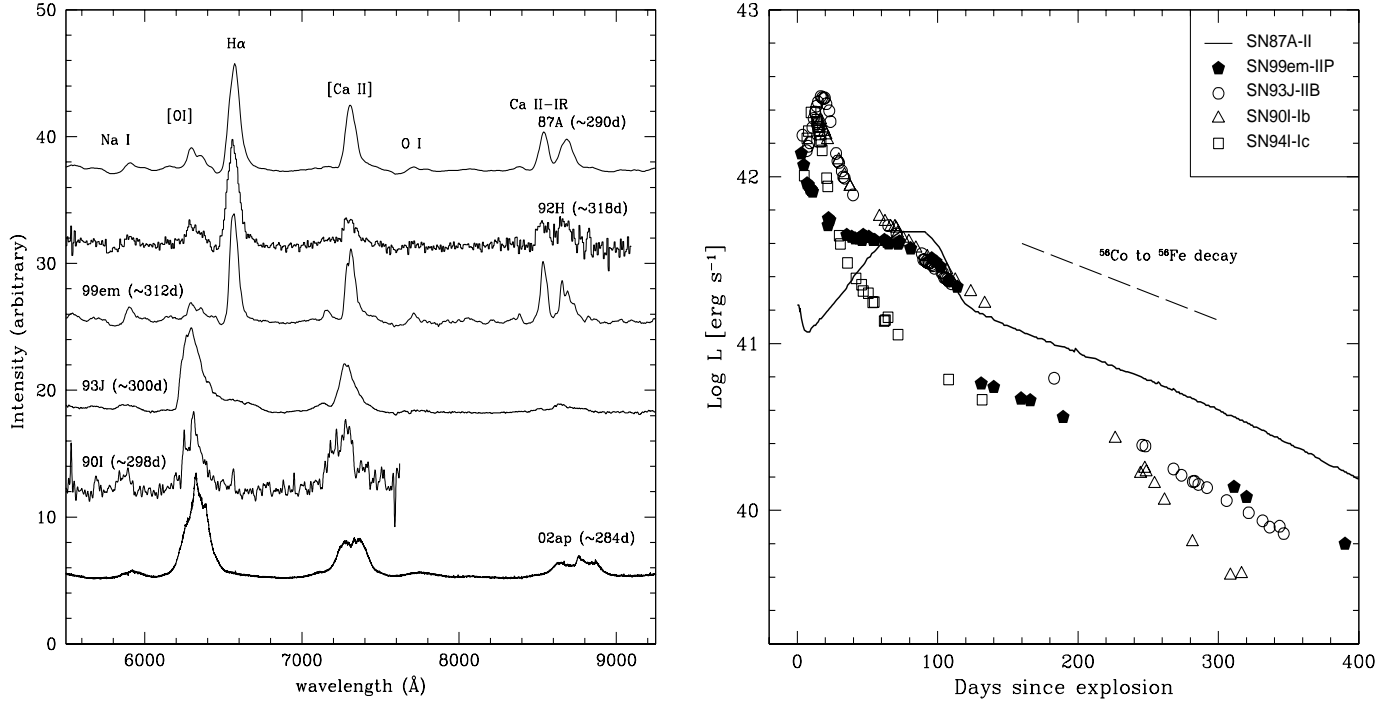


Fig. 1. *Left panel*: a sample of the late time CCSNe spectra. The most prominent lines are labeled. The corresponding observation date, since explosion time, are also reported. *Right panel*: the computed quasi-bolometric light curve of SN II 1987A (UBVRI bands); SN IIP 1999em (UBVRI-bands); SN Ib 1990I (BVRI-bands); SN Iib 1993J (UBVRI bands) and SN Ic 1994I (BVRI bands). The ⁵⁶Co to ⁵⁶Fe decay slope is also shown for comparison.

discussed. The [O I] 6300,6364 Å line luminosity and the F_{6300}/F_{6364} flux ratio are measured and presented in Section 3. In Section 4, we discuss two different methods for estimating oxygen mass in CCSNe. The methodology of ⁵⁶Ni mass estimation is given. We also evaluate the integrated flux ratio of the forbidden emission lines [Ca II] 7291,7324 Å and [O I] 6300,6364 Å. We conclude with a summary and discussion of our findings in Section 5.

2. The sample

The selected sample consists of 26 CCSNe objects – 13 of them are type II, one of type Iib and 12 of type Ib-c. Data are gathered mainly from the literature (i.e. published available data). Use is made of the “SUSPECT”¹ and of the “CfA”² Supernova Spectra Archives. Some measurements are made on late spectra of SN 1996aq, taken from the Padova-Asiago supernovae database. A summary of refer-

¹<http://bruford.nhn.ou.edu/~suspect/index1.html>

²<http://cfa-www.harvard.edu/oir/Research/supernova/SNarchive.html>

ences and descriptive parameters of individual objects is given in Table 1.

In what follows we adopt the standard reddening laws of Cardelli et al. (1989).

An example of the analyzed late spectra is shown in Fig.1(left panel), together with identifications of the most prominent lines. We focus on the wavelength range 5500-9200 Å. At this epoch, when the events are in the radioactive tail phase, and except for the notable H α emission in type II SNe, the optical spectra are dominated by emission lines of [O I] 6300,6364 Å, [Ca II] 7291,7324 Å and Ca II-IR triplet. The emission centered at $\lambda \sim 7800$ Å is usually attributed to O I 7774 Å. These aspects will be highlighted when evaluating the [O I]/[Ca II] line intensity ratio of the sample objects.

Worth recalling here that the [O I] 6300,6364 Å line is found to be absent or very weak in SNe of type IIn³.

In Fig.1 (right panel) the constructed “quasi-bolometric” light curves of SNIIP 1999em, SNIib 1993J, SNIb 1990I and SNIc 1994I are displayed. The peculiar SNII 1987A is also included for comparison. The available optical “U,B,V,R,I” broad-band photometric data have been integrated to recover the pseudo bolometric light curves. Literature references for the photometry, together with the adopted parameters are reported in Table 1. We do not include the IR-contribution since it is available only for SN 1987A, and hence the derived integrated bolometric light curves represent a lower limit to the “real” bolometric light curves. The ⁵⁶Co to ⁵⁶Fe decay slope, e —folding time of 111.3 days, corresponding to the full γ —ray trapping is also shown.

The difference in the early CCSNe bolometric light curves, i.e. the peak in type Ib-c SNe and the plateau in type II SNe, is mainly related to differences in presupernovae radii and structures. The plateau behaviour in type II is indicative of massive hydrogen envelopes, although its properties (duration and luminosity) predict also a dependence on radius, energy and the ejected amount of ⁵⁶Ni (Popov 1993; Elmhamdi et al. 2003). The lack of such significant hydrogen in the outer layers of type Ib-c inhibits the presence of a plateau behaviour.

The peak characteristics, luminosity and width, are sensitive to the ejecta mass, released energy and the ⁵⁶Ni mass (Arnett 1982).

The clear faster decline at late phases for type Ib-c SNe is naturally attributed to the significant γ -ray escape with decreased deposition as a result of low mass ejecta in this class of objects, while owing to the massive hydrogen mantle, type II SNe light curves indicate that radioactive decay of ⁵⁶Co with the consequent trapping of γ -rays is the main source of energy powering the light curves at late times. We note

³“n” stands for narrow. Type IIn are characterized by a narrow H α emission and high bolometric light curve with a relatively flat evolution. In the prototype SN IIn 1988Z indeed there was no sign of the nebular forbidden lines [O I] 6300,6364 Å and [Ca II] 7291,7324 Å. Similar behaviour is observed in SN IIn 1994aj (Benetti et al. 1998). The well studied events SN IIn 1995N (Fransson et al. 2002; Pastorello et al. 2005) and SN IIn 1995G (Chugai & Danziger 2003; Pastorello et al. 2002) display the same characterizing peculiarity. One possibility for this is that their progenitors are not massive, believed to explode in a very dense CS environment.

that in type II objects the V-light curve follows the bolometric light curve fairly well at late epochs, which simplifies for example the derivation of the synthesized ^{56}Ni mass. It is sufficient then the use of the tail absolute V-light curve of SN 1987A, for which the ejected ^{56}Ni mass is accurately known from observations and detailed modeling, as a template for ^{56}Ni mass derivations in other II events (Elmhamdi et al. 2003b; Hamuy 2003). The stripped-envelope SNe case is more difficult. The V-band light curve does not parallel the bolometric one. It is hence necessary in type Ib-c a bolometric light curve modeling rather a simple use of the absolute visual bands.

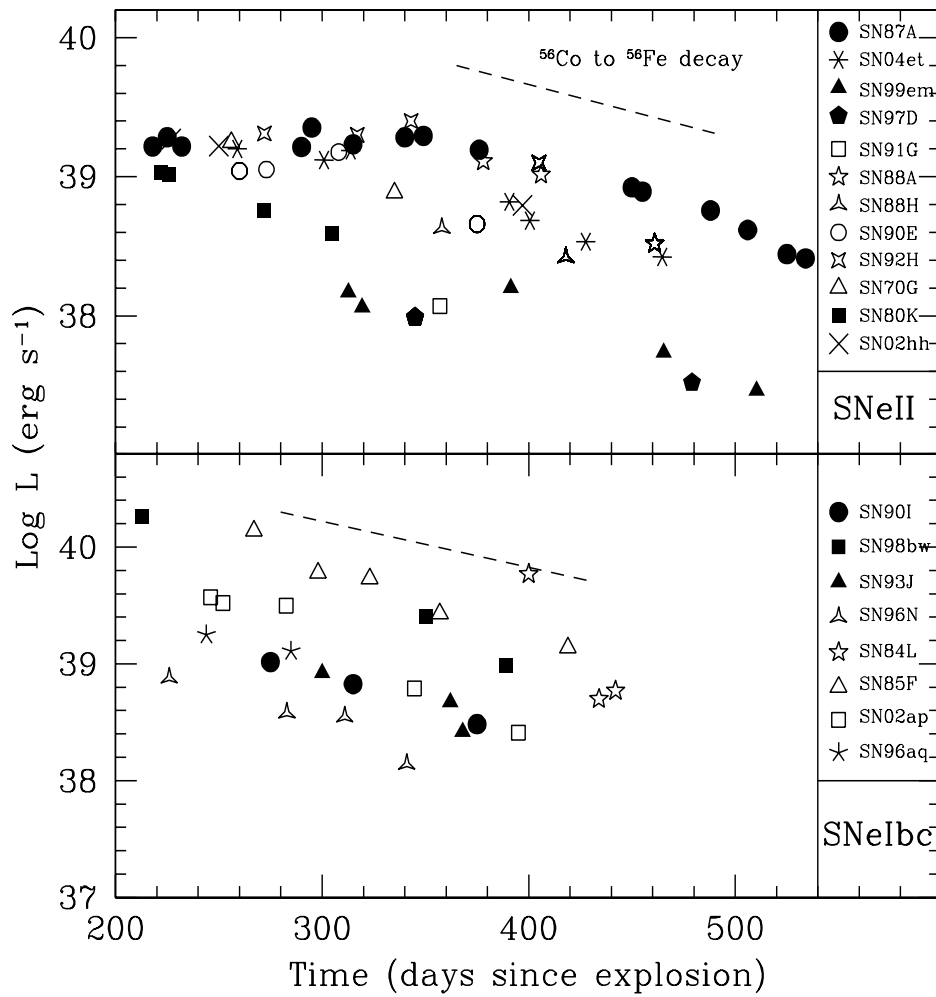


Fig. 2. The temporal evolution of the [O I] 6300,6364 Å luminosity for SNe of type II (upper panel) and for SNe Ib-c (lower panel). The ^{56}Co to ^{56}Fe decay slope is also reported.

3. The analysis

In this section we measure and study the oxygen [O I] 6300,6364 Å line luminosity for the CCSNe sample. For this purpose the available spectra were corrected for redshift and reddening effects and calibrated with photometry when needed. The recovered integrated line fluxes, assuming a continuum level, are then converted to luminosities using adopted distances.

3.1. Oxygen Luminosity and Mass

3.1.1 The luminosity

Figure 2 highlights the [O I] 6300,6364 Å line luminosity temporal evolution, starting at 200 days after explosion, for type II SNe (upper panel) and for type Ib-c SNe (lower panel). For comparison, the ^{56}Co to ^{56}Fe decay slope is also displayed (for an arbitrary ^{56}Ni mass; dashed line).

The emission [O I] 6300,6364 Å light curves behave differently within the CC-SNe family. For type II events: the light curves have a plateau-like maximum at day 200, changing slowly until day ~ 340 . At this epoch the light curves are already on the exponential decline phase (Fig.1-right panel). The line-luminosity dropped then sharply, with a rate of decrease similar to that of the radioactive decay of ^{56}Co (i.e. e -folding time of 111.3 days). We note here that in the case of SN 1987A, it has been argued that dust condensation affects the line luminosity evolution starting at day ~ 530 , inducing a further increase in the rate of decrease (Danziger et al. 1991). At approximately the same time the [O I] line profile showed a marked shift of the peaks towards blue wavelengths (Lucy et al. 1989). There are however two exceptions decaying earlier compared to the rest of the II SNe sample, namely SN 1970G and SN 1980K. Interestingly these two objects are respectively type IIP-L and IIL SNe. For type Ib-c events: starting at the age of 200 days, the light curves are already on a steep decline, faster to that of the ^{56}Co radioactive decay. The “Chi Square” fit to SN Ib 1985F luminosity data for example indicates an e -folding time of about 70 days. The time at which the deviation to the decline occurs varies among the CCSNe family, being earlier in Ib-c, followed by IIL and then later on SNe IIP. Specifically the line luminosity trend is found to follow the bolometric light curves in the time range of interest, namely after 200d in type Ib-c and after ~ 340 d in type II. In SN 1987A for example, the [O I] luminosity relative to the bolometric one, i.e. $(L_{[\text{OI}]} / L_{\text{bol}})$, shows an almost flat-topped behaviour at the time interval $\sim 340 - 500$ d. Other effects enter at later epochs, > 500 d, such as dust condensation and the IR-catastrophe (Danziger et al. 1991; Fransson et al. 1996; Menzies 1991). On the one hand this is a direct evidence that the dominant source of ionization and heating is γ -rays from the radioactive decay of ^{56}Co in the CCSNe variety, with the γ -rays escaping with decreased deposition in type Ib-c events, owing to the low mass nature of their ejecta. We note also that in both panels the line light curves span more than one dex in luminosity, which may be

related to the variation in the oxygen yields. Thus the importance of the oxygen mass estimates.

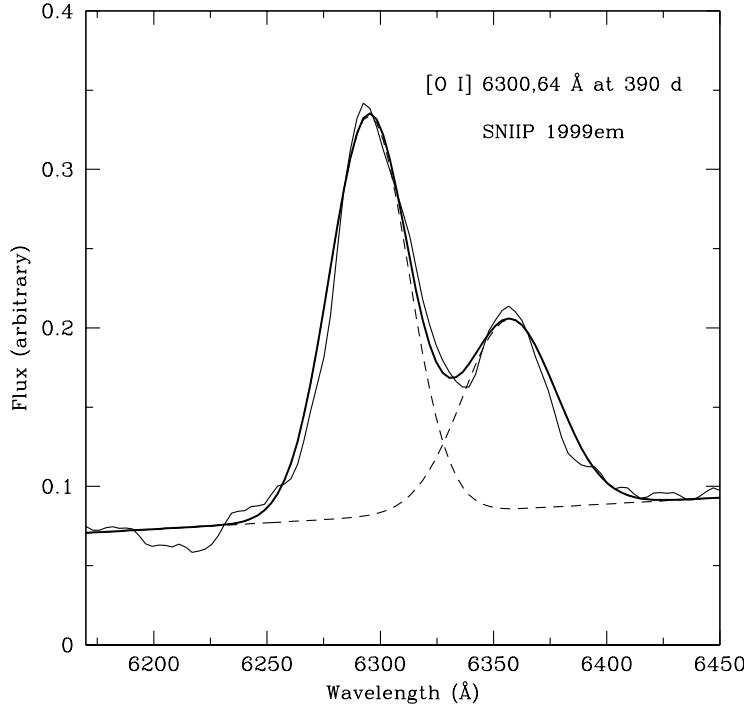


Fig. 3. The fit example to the [O I] 6300,6364 Å profile of SN IIP 1999em at day 390. Shown in thick line is the best fit. Dashed profiles refer to the decomposition of the best fit into two Gaussians for the [O I] 6300 Å and [O I] 6364 Å components.

3.1..2 The flux ratio “ F_{6300}/F_{6364} ”

Various investigators have dealt with the doublet flux ratio in the [O I] 6300,6364 Å line, especially for the well observed SN 1987A (Spyromilio & Pinto 1991; McCray 1996). It is well established that for a large and homologously expanding atmospheres such as in supernovae events, the Sobolev approximation holds and consequently simplifies the radiation transfer and line formation treatments (Castor 1970; Jeffery & Branch 1990).

Within this context, a line intensity is given by: $Flux \propto P_{esc} \times A_{ul} \times N_u$, where N_u is the number density of atoms in the upper state, A_{ul} is the Einstein coefficient, and P_{esc} being the escape probability giving by $P_{esc} = [1 - \exp(-\tau)]/\tau$; τ is the Sobolev optical depth. For a freely expanding atmosphere the density N_u goes as t^{-3} and hence the Sobolev optical depth should behave as $\tau \propto N_u \times t = t^{-2}$.

For the line of interest, i.e. the [O I] 6300,6364 Å doublet, the two transitions have $A_{6300} = 3 \times A_{6364}$, and $\tau_{6300} = 3 \times \tau_{6364}$; therefore the doublet flux ratio reads:

$$\frac{F_{6300}}{F_{6364}} = \frac{1 - \exp(-\tau_{6300})}{1 - \exp(-\tau_{6364})} = \frac{1 - \exp(-\tau_{6300})}{1 - \exp(-\tau_{6300}/3)} \quad (1)$$

A measure of the flux doublet ratio can be then translated into the optical depth in the 6300 Å line in the SNe ejecta through solving Eq. 1. In addition we expect an asymptotic value for the ratio to be 1 for the optically thick transitions and to be 3 for the optically thin case.

Recovering the ratio of the flux doublet is not always an easy task. Line blending can prevent an adequate intensity measurement. One possibility is a simple use of the peak intensities in the components of the doublet assuming it similar to the ratio of the flux of the doublet components (Li & McCray 1992). Deblending yields to more accurate line ratio determination, especially in cases with a sever blend. We selected a variety of objects within our CCSNe sample that allow good estimates of the ratio. The studied events are: SNe IIP(1988A, 1999em, 2004et), SNe Ib(1985F, 1990I) and SNe Ic(1998bw, 2002ap). Data for SN 1987A are also included for comparison. An example is illustrated in Fig.3 for the observed spectrum of SN IIP 1999em at day 390. Our adopted methodology consists in fitting the [O I] 6300,6364 Å feature with a single function formed by 2 Gaussians, after estimating the continuum level and fixing the wavelength separation of the doublet, i.e. 64Å, and with both Gaussians having the same velocity width. The fit in Fig.3 is a good one. In some cases it was not possible to obtain a particularly good overall fit using only two Gaussians since one is left with either a residual in the blue wing of the 6300 Å component for narrower lines, or little evidence of the the 6364 Å component for broader lines. Elmhamdi et al. 2004 have used similar methodology and obtained a satisfactory fit in the spectrum of SN Ib 1990I at 254d introducing a third Gaussian component assuming there is a contribution from Fe II 6239 Å emission, and allowing its velocity width to be a free parameter (their Fig. 7). According to our sample analysis the two approaches, using the deblending technique and a simple use of the peak fluxes, when possible, agree within 20%. Figure 4 reports the results of our investigation. The upper panel displays the temporal evolution of the ratio measurements, while in the lower panel we plot the corresponding optical depths in the primary component, computed by solving Eq. 1. The ratio values demonstrate a temporal trend from an optically thick phase to an optically thin one. The optical depth is found to decrease from values as high as ~ 7 around day 170 falling to lower values at later phases (< 0.5 around 500d). The continuous line is the resulted LSQ fit to the data, using a power-law function (i.e. $\propto t^{-n}$). The best fit gives an index of $n = 2.089 (\pm 0.153)$. This is consistent with the index expected from the simple expansion assumption discussed above (i.e. $\tau \propto N_u \times t = t^{-2}$).

Furthermore, we may introduce a time dubbed t_{trans} , as the time at which the line makes the transition to the phase characterized by $\tau_{6300} = 1$. In fact using

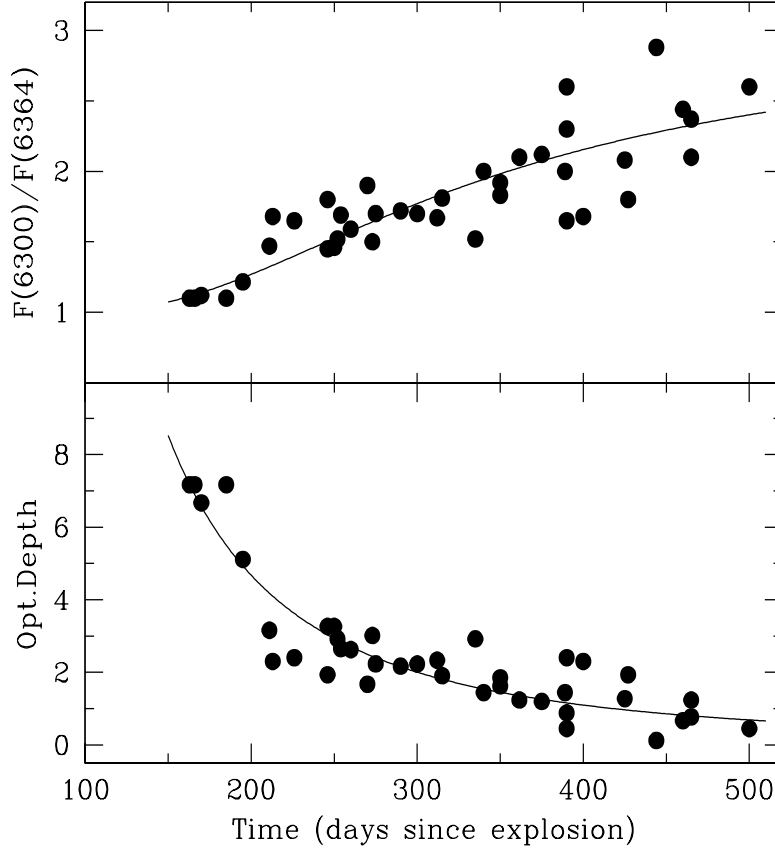


Fig. 4. *Upper panel*: the temporal evolution of the flux ratio F_{6300}/F_{6364} . The overplotted curve corresponds to the LSQ-fit by Eq. 2, indicating a value of $t_{trans} \simeq 426$ d (see text for details). *Lower panel*: the recovered optical depths in the [O I] 6300Å line. The power law LSQ-fit is also displayed ($\sim t^{-n}$ with $n = 2.089 \pm 0.153$; see text).

$\tau \propto t^{-2}$ and introducing t_{trans} , Eq. 1 can be written as:

$$\frac{F_{6300}}{F_{6364}} = \frac{1 - \exp(-(t_{trans}/t)^2)}{1 - \exp(-(t_{trans}/\sqrt{3}t)^2)} \quad (2)$$

Provided the ratio measurements, we fit the data with Eq.2. The LSQ fit is shown by the continuous line in the upper panel of Fig. 4. The best fit indicates a time of $t_{trans} = 426.06 \pm 13.24$ d. The time at which $\tau_{6364} = 1$, is 245.96 ± 7.64 d.

This above described analysis demonstrates the consistency within the CCSNe family on how the components intensity ratio and the optical depths develop in time.

3.1.3 The mass

In this section we adopt two different methods for estimating the oxygen mass in SNe of type II and SNe of type Ib-c.

- *Type II SNe:*

We use the recovered [O I] doublet luminosities to determine the abundance of the oxygen produced through the SN explosion.

At the epoch of about 1 year, the luminosity of the [O I] doublet is powered by the γ -ray deposition and by ultraviolet emission arising from the deposition of γ -rays in oxygen material. The [O I] doublet luminosity is related directly to the oxygen mass (Elmhamdi et al. 2003a), and at a given time one may write:

$$L_t([\text{O I}]) = \eta \times L_t(^{56}\text{Co}) \times \frac{M_{\text{O}}}{M_{\text{ex}}} \quad (3)$$

where M_{O} is the mass of oxygen, M_{ex} is the “excited” mass in which the bulk of the radioactive energy is deposited, and η is the efficiency of transformation of the energy deposited in oxygen into the [O I] doublet radiation. The $L_t(^{56}\text{Co})$ refers to the radioactive decay energy input, given by $L_t = L_0 \times (M_{\text{Ni}}/M_{\odot})e^{-t/\tau_{\text{Co}}}$, with $L_0 \simeq 1.32 \times 10^{43} \text{ ergs s}^{-1}$, the initial luminosity corresponding to $1 M_{\odot}$ and $\tau_{\text{Co}} = 111.3 \text{ d}$.

Assuming then that all type II events have similar η and M_{ex} at similar phases, we derive rough estimates of the oxygen mass for the events of the sample adopting [O I] 6300,6364 Å light curve of SN 1987A as template. As discussed previously, the [O I] luminosity is found to have similar decay rates in SNe II at late phases, following a behaviour similar to the bolometric light curves. This fact gives some confidence for the use of SN 1987A [O I] luminosity as a template for the recovery of the amounts of ejected oxygen. The oxygen mass in SN 1987A is estimated to be in the range $1.5 - 2 M_{\odot}$ (Fransson et al. 1996; Chugai 1994).

In Table 1, column 7, we report the amounts of the ejected oxygen mass derived in this manner. The variation range, for each event, reflects the combination of the variation in the oxygen mass for SN 1987A (i.e. $1.5 - 2 M_{\odot}$) together with the uncertainties from the fit procedure.

- *Type Ib-c SNe:*

The emission lines which are formed at densities above their critical ones, given the optical depths are not large, have the luminosity directly proportional to the mass of the emitting ion. Such conditions hold for the [O I] 6300,6364 Å doublet line emission in type Ib-c SNe at nebular phases. On the one hand, we found moderate optical depths at late phases (Fig 4, lower panel). On the other hand, the condition of the high density limit above the critical density for the [O I] line ($\sim 7 \times 10^5 \text{ cm}^{-3}$) is found to be clearly fulfilled in the ejecta of type Ib-c SNe (Leibundgut et al. 1991; Elmhamdi et al. 2004). A possible direct method can be

used to check the high density limit characteristic. Indeed, the density is directly related to the relative strengths of the [O I] doublet components (Leibundgut et al. 1991; Spyromilio & Pinto. 1991). In both cited works, the variation of the line doublet ratio as function of the density at a given time is computed, and is found to be insensitive to the adopted temperature, especially for the late epochs. From our computations we take a ratio value of 1.58 at day 250 or 1.8 at day 300 as representatives (i.e. from the best fit in Fig.4-upper panel). According to Fig. 6 of Leibundgut et al. (1991), the uncertainty in the temperature leads to the following density range $2 \times 10^9 \text{ cm}^{-3} \leq N_e \leq 4 \times 10^9 \text{ cm}^{-3}$.

In the high density limit, i.e. above the critical density, the mass of ejected oxygen can be recovered using the [O I] 6300,6364 Å flux. Uomoto (1986) has shown that the oxygen mass, in M_\odot , is given by:

$$M_{\text{Ox}} = 10^8 \times D^2 \times F([\text{O I}]) \times \exp(2.28/T_4) \quad (4)$$

where D is the distance to the supernova (in Mpc), F is the reddening-free [O I] integrated flux (in $\text{ergs s}^{-1} \text{ cm}^{-2}$) and T_4 is the temperature of the oxygen-emitting gas (in 10^4 K).

Worth noting that because of the variation of $F([\text{O I}])$ and T_4 , Eq. 4 implies time-dependence. Schlegel & Kirshner (1989), when estimating the ejected oxygen amounts, have adopted a constant temperature $T_4=0.4$ at the nebular phase of SNe Ib 1984L and 1985F. The assumption of a constant temperature at different late phases provides different oxygen masses as one may expect, since earlier nebular epochs are hotter compared to latter ones.

Alternatively, the temperature at a given time can be constrained based on the [O I] 5577 Å to [O I] 6300,6364 Å flux ratio. Assuming that the O I lines are formed mainly by collisional excitation, the ratio is given by the following expression (Houck & Fransson 1996):

$$\frac{F_{6300}}{F_{5577}} = 0.03\beta_{6300} \times [1 + 1.44T_3^{-0.034}(\frac{10^8}{N_e})] \times \exp(25.83/T_3) \quad (5)$$

where T_3 is the temperature of the oxygen-emitting gas (in 10^3 K), β_{6300} is the [O I] 6300 Å Sobolev escape probability ($\simeq 1$) and N_e is the electron density.

A problem with this method is the very weak observed [O I] 5577 Å feature in the late time spectra analyzed here. It is indeed an indication of low temperatures in the oxygen-emitting zone. However one may estimate an upper limit on the [O I] 5577 Å flux by integrating over the same velocity interval of the [O I] 6300,6364 Å profile. It is found that the temperatures at late phases of interest, $\geq 250\text{d}$, tend to have values in the range 3400 – 4200 K.

Results from this described method, through equation 4, are listed in column 7 in Table 1. For SNe 1994I, 1993J, 1998bw and 2002ap however, the amounts

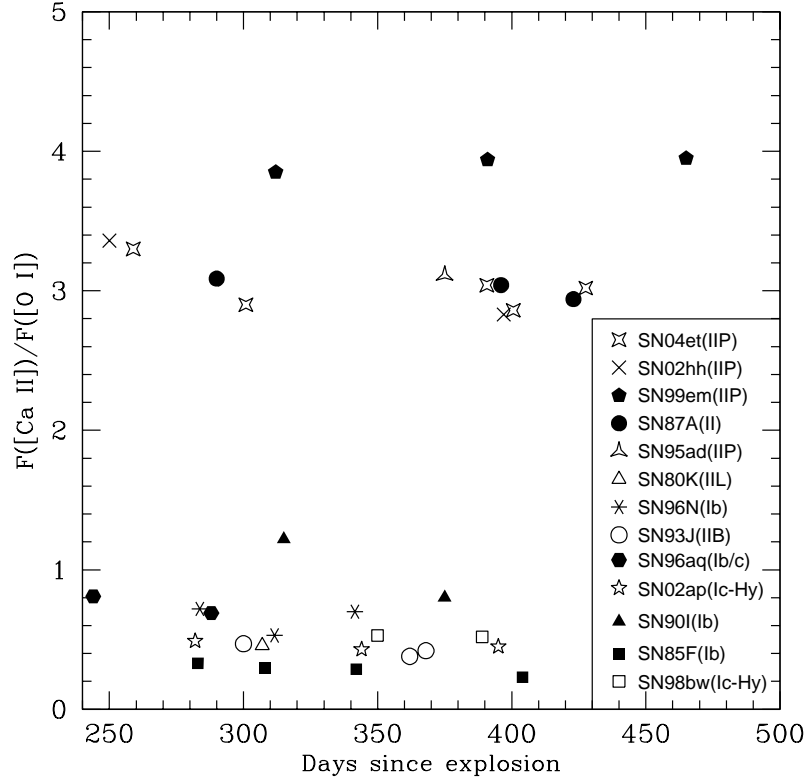


Fig. 5. The temporal evolution of the [Ca II] 7291,7324 Å over [O I] 6300,6364 Å integrated flux ratio. Note the complete separation of type Ib-c from type II SNe.

reported in the table come from the most recent spectroscopic and photometric modeling (see column 8 for references).

3.1.4 The [Ca II]/[O I] intensity ratio

After considering the reddening correction, we have evaluated the integrated flux ratio of the forbidden emission lines [Ca II] 7291,7324 Å and [O I] 6300,6364 Å, for the CCSNe sample objects having wavelength coverage in these two nebular lines. Results are displayed in Fig. 5. Two separate populations are clearly distinguishable. The ratio is found to remain below unity in type Ib-c, with the exception of SN 1990Ib around day 315 (~ 1.22). SNe IIb 1993J, Ic-hypernova 1998bw and IIL 1980K belong to this category as well. A mean value is measured to be ~ 0.51 . SNe of type II instead concentrate on the top of the figure, with a mean value of ~ 3.17 . Additionally, the two classes appears to have a flat evolution behaviour of the [Ca II]/[O I] ratio.

In a detailed analysis, Fransson & Chevalier (1987, 1989) have modeled late emission spectral lines for different supernova progenitors. It is found that be-

cause of the composition and density structures one can use the relative emission line strengths as a progenitor indicator tool. In particular the forbidden emission line ratio $[\text{Ca II}]/[\text{O I}]$ presents weak dependence on density and temperature of the emitting zones, and is expected to display an almost constant evolution at late epochs. The ratio is found to be very sensitive to the core structure and mass. Furthermore it seems that the ratio tends to increase with decreasing progenitor mass. The distribution of our measurements in two groups tend to indicate different progenitor properties, with lower progenitors for type Ib-c, IIb and IIL classes compared to normal type IIP events. It is worth to note here however that in type Ib-c SNe there is no hydrogen rich Ca II emitting zone as is the case for type II objects (de Kool et al. 1998).

3.1..5 The ^{56}Ni mass

As discussed in Sect. 2, the exponential behaviour of the late V-band absolute light curves of type II SNe is found to be in accordance with the radioactive decay $^{56}\text{Co} \rightarrow ^{56}\text{Fe}$ ($M_V \propto \exp(-t/111.3 \text{ d})$), which provides a potential method to recover the amount of the ejected ^{56}Ni with the use of the M_V photometry of SN 1987A as a template between 120 – 400 d (Elmhamdi et al. 2004; Hamuy 2003). An amount of $0.075 M_\odot$ is adopted for the ^{56}Ni mass of SN 1987A (Catchpole et al. 1988, Suntzeff & Bouchet 1991). Results from the described methodology are reported in Tab. 1 (column 6). There is a significant scatter of the ejected ^{56}Ni masses, with an average value of $\approx 0.053 M_\odot$.

For type Ib-c events, the broad band light curves do not trace necessarily the bolometrics. The amounts summarized in Tab. 1(column 6) are indeed results from bolometric light curves and/or spectra modeling (see column 8 for the corresponding references). An average value of $\approx 0.18 M_\odot$ is computed.

4. Discussion and conclusions

We have selected a sample of 26 events within the CCSNe family. Our main goal was to investigate how the oxygen manifests its presence at late phases for each SN class, especially the emission $[\text{O I}]$ 6300,6364 Å doublet.

Based on investigating early spectra of CCSNe, the permitted oxygen line O I 7773 Å seems to get weaker following the SNe sequence “Ic – Ib – IIb – II” (Elmhamdi et al. 2006; Matheson et al. 2001). For stripped envelope objects, being less diluted by the presence of an helium envelope, one may expect the oxygen lines to be more prominent. An observational fact that clearly support this belief is the earlier appearance of the $[\text{O I}]$ 6300,6364 Å following the above order, i.e. “Ic – Ib – IIb – II”. The following examples highlight this fact. The oxygen line emerges at an age of 1-2 months in type Ic SN 1987M (Filippenko 1997). SN Ic 1994I displayed evidence for the line at an age of 50 days, although some hints may even be seen in the ~ 36 days spectrum (Clocchiatti et al. 1996b). SN Ic 1997B

shows clear evidence for [O I] 6300,6364 Å, [Ca II] 7291,7324 Å and also O I 7773 Å on the 2 months spectrum (Gomez & Lopez 2002). In SN 1998bw, Ic-hypernova event, the nebular features were already recognizable in the 43 days spectrum (Patat et al. 2001). While in SN Ib 1990I it was hinted at the 70 days spectrum (Elmhamdi et al. 2004). In other type Ib SNe it appears earlier than in SN 1990I. In SN Iib 1993J, a transition object, the line was visible in the 62 days spectrum (Barbon et al. 1995). SN 1996cb, another well observed Iib event, showed evidence of the [O I] 6300,6364 Å line around day 80 (Qiu et al. 1999). In SNe II, however, the line appears later: around day 150 in SN 1987A (Catchpole et al. 1988) and after day 138 in SN 1992H (Clocchiatti et al. 1996a). In SN II 1999em it is suggested at a somewhat earlier phase compared to SNe 1987A and 1992H, namely at day 114.

Furthermore, the width velocities in the [O I] 6300,6364 Å and in the [Ca II] 7291,7324 Å nebular lines are mainly found to be higher in SNe Ic than in SNe Ib (Schlegel & Kirshner 1989; Matheson et al. 2001). In the cited papers, the FWHM values were evaluated fitting a single profile, namely Gaussian, to the total observed profiles. We mention here that given the line blending in these two lines (doublets), results should be interpreted with some caution. One should indeed resolve the lines and compare width velocities of single components rather than using a single Gaussian fit to the whole feature. It is not simple however in some cases to get a satisfactory fit, especially when the blend is sever. According to our analysis, we faced more difficulties in type Ib and Ic than in type II. This fact is indeed in itself indicative of higher velocities in stripped envelope objects, while in SNe II, owing to lower expansion velocities, the observed [O I] 6300,6364 Å profile is less complex and the two components are clearly visible. This can be easily understood if considering the formation of the line doublets in cases where the element expansion velocity does not exceed the the two components separation velocity, i.e. 3000 km s^{-1} . We have checked the width velocities by means of the FWHM of the single [O I] component at 6300 Å of some of our sample events. At a phase of $\sim 300\text{d}$, SNe II 1987A and 1999em are found to have respectively FWHM ([O I] 6300) ~ 2750 and 2400 km s^{-1} , while for Ib SNe a typical range variation of $\sim 4000 - 5000 \text{ km s}^{-1}$ is deduced (e.g. SNe Ib 1985F, 1996N). SN Iib 1993J, at similar age, has a velocity of $\sim 4600 \text{ km s}^{-1}$, with a complex [O I] 6300,6364 Å profile due to the presence of $\text{H}\alpha$ at the red wing of the line (Patat et al. 1995). Higher velocities, $\geq 6000 \text{ km s}^{-1}$, are computed from Ic spectra (e.g. SNe 1987M, 1994I and 1998bw). The [O I] 6300,6364 Å nebular line at late epochs is representative of the expansion velocity. For a given explosion energy, a greater ejecta mass allows for lower velocities. The found lower velocities in type II SNe can be attributed then to a large mass with respect to type Ib-c objects.

We have investigated in details the properties of the [O I] 6300,6364 Å doublet profile. The measured line luminosities are found to trace well the bolometric light curves, behaving differently in type Ib-c than in type II events. In SNe II, the line light curves show a plateau-like evolution until ~ 340 days, following later-on by

an exponential decline similar to the radioactive decay of ^{56}Co (e -folding $\simeq 111.3$ days). The linear type II SNe display an early decline in their [O I] light curves. type Ib-c light curves display already a decline by an age of 200 days, steeper than the ^{56}Co radioactive decay rate. The γ -rays from the radioactive decay of ^{56}Co are hence the dominant source of ionization and heating in CCSNe variety. Furthermore, owing to the low mass nature of their ejecta, type Ib-c SNe are characterized by a decreasing deposition of the γ -rays escape. Similar conclusions about the progenitor diversity are argued from the analysis of the integrated flux ratio of the forbidden emission lines [Ca II] 7291,7324 Å and [O I] 6300,6364 Å. The ratio is found to concentrate in two distinguishable locations, namely around a value of 3 for type II SNe (mean ~ 3.17), and below unity in Ib-c objects (mean ~ 0.51). This forbidden lines ratio is potentially sensitive to the progenitor mass star (Fransson & Chevalier 1987; 1989), suggesting higher masses in SNe of type II.

The way CCSNe family members transit from optically thick to optically thin phases is imprinted onto the profile of the [O I] 6300,6364 Å doublet. We emphasize this point making use of the components flux ratio F_{6300}/F_{6364} , after deconvolving the two components of the observed line profiles. Based on a simple description of the physics behind the line formation, our results indicate a consistency within the CCSNe on how the components intensity ratio and consequently the optical depths develop in time. Additionally, the ratio F_{6300}/F_{6364} can be used to estimate the average density of the oxygen-emitting zone (Leibundgut et al. 1991; Spyromilio & Pinto 1991). Adopting representative values of the ratio of 1.58 at day 250 or 1.8 at day 300, inferred from our best fit in Fig.4-upper panel, and according to Fig. 6 of Leibundgut et al. (1991), the uncertainty in the temperature leads to the following density range $2 \times 10^9 \text{ cm}^{-3} \leq N_e \leq 4 \times 10^9 \text{ cm}^{-3}$. Worth noticing here that based on our approach one may get further informations about the physical conditions in the oxygen emitting region. In fact, for an uniform density distribution, one may use the above derived density range together with the element volume, based on the [O I] 6300 Å FWHM velocity, to get a rough estimate of the ejected oxygen mass. This approach is found to provide too large amounts compared to results reported in Tab. 1 (column 7). For SN IIP 1999em for example, at 300 days, using the previous derived velocity of 2400 km s^{-1} , we find an ejected oxygen mass as high as $\sim 40 M_{\odot}$, indicating a volume-filling factor as low as 10^{-2} . Similar filling factor is found for SN II 1987A and SN Ib 1990I. These results suggest that the oxygen material in CCSNe generally fills its volume in a clumpy way rather than homogeneously.

We describe and adopt two methods for the oxygen mass estimate in CCSNe. We provide also estimates of the ejected ^{56}Ni masses. It should however be noted that various parameters affect the recovered values, especially as long as the oxygen mass is concerned, contributing hence to their uncertainties. Indeed, the luminosity and temperature measurements are sensitive to the nature and quality of the spectra (i.e. severe line blending; multi-component profiles; presence of [O I] 5577 Å).

According to our test effects, we estimate the uncertainty of the derived oxygen-mass amounts reported in Tab. 1 to vary within 15 – 30%. Furthermore, for cases with clear evidence of O I 7774 Å line, the presence of ionized oxygen is argued (Mazzali et al. 2010), requiring higher mass of oxygen than the one needed to produce [O I] 6300,6364 Å alone. Generally, Nickel masses are found to suffer less uncertainties compared to oxygen. The errors in type II SNe, being more homogeneous than SNe Ib-c, do not exceed 20% (mainly due to distance and reddening estimates). In SNe Ib-c, we estimate a variation of 10 – 30%.”

These estimates, i.e. oxygen and iron masses, are of importance as they can be indicative of the core mass and related to the progenitor star nature. For the purpose of a better investigation, we compute the $[O/Fe]^4$ yields ratio for each event. A solar value of $\log_{10}(O/Fe)_{\odot} = 0.82$ dex (Anders & Grevesse 1989) is adopted. The recovered amounts are reported in Fig. 6 (horizontal lines) as function of the initial mass according to the most reliable core collapse SN models in literature, namely Woosley & Weaver 1995 (short dot-dashed line), Thielemann, Nomoto & Hashimoto 1996 (long dashed line) and Nomoto et al. 1997 (long dot-dashed line). A typical value for type Ia SNe is as well reported (Nomoto et al. 1984), which shows the nature of type Ia SNe being iron producers.

Fig. 6 defines two possible concentration regions, of type II objects from one side and type Ib-c from the other side, and suggestive of a continuum in the $[O/Fe]$ values. Indeed, an important issue that can be read out immediately from Fig. 6 is that the reported results for type Ib-c are found to be located at the bottom of type II SNe. These zones may provide constraints on the progenitor masses in CCSNe family. Within the core collapse models of type Ib-c SNe, two scenarios are argued: *first* a single high mass star ($M_{ms} \geq 35 M_{\odot}$) exploding as Wolf-Rayet star after an episode of strong stellar wind, and *second* a less massive star ($M_{ms} \sim 13 - 18 M_{\odot}$) in a binary system. Although the progenitor nature of type Ib-c SNe is an open and debated issue, the position of type Ib-c events in the “ $[O/Fe]$.vs. M_{ms} ” plot, according to Fig. 6, might be taken as an observational support of the intermediate massive stars in binary systems, stripped of their envelope through binary transfer, as the favoured progenitors in this class of objects.

Although the uncertainties in the stellar evolution models of massive stars and in the determination of the oxygen and iron yields, Fig. 6 provides a methodology to elucidate the progenitor nature of core collapse SNe and interesting comparisons can be drawn. However, extended samples and more reliable determinations, especially for oxygen abundances (late spectra modeling for example), are clearly needed to populate the “ $[O/Fe]$.vs. M_{ms} ” diagram and hence have a deeper view on the oxygen to iron ratio and how it changes as function of the type of SN. The present quantitative analysis can also provide insights and input data for the evolution of galaxies and the chemical enrichment models.

The main goal of the paper was to highlight some late-phases spectra related

⁴ $[A/B] = \log_{10}(A/B)_{\star} - \log_{10}(A/B)_{\odot}$

properties of CCSNe, providing possible physical interpretations. As a first step we concentrate our study on 26 selected events. For future investigation we aim to enlarge the studied sample including more recent and up-dated observed CC-SNe objects, especially those with spectra of improved time coverage and spectral resolution (mostly last decade observations; Elmhamdi et al. In preparation).

Acknowledgements. We thank the referee for the very helpful and constructive suggestions. We thank I. John Danziger for his comments on the original manuscript and for the stimulating discussions. We are grateful for the use of the “SUSPECT” SNe Archive-Oklahoma University and also of the “CfA” Supernova Archive. We also thank D. K. Sahu for providing published data of SN IIP 2004et, R. Foley for the discussion about SN Ic 2002ap data and M. Pozzo for discussing SN IIP 2002hh. This project was supported by King Saud University , Deanship of Scientific Research, College of Science Research Center.

REFERENCES

- Anders E. & Grevesse N. 1989, *Geochimica et cosmochimica Acta*, **53**, 197.
 Arnett W. D. 1982, *ApJ*, **253**, 785.
 Barbon R., Ciatti F. & Rosino L. 1973, *A & A*, **29**, 57.
 Barbon R. et al. 1995, *A & AS*, **110**, 513.
 Baron E., Branch D, Hauschildt P. et al. 2000, *ApJ*, **545**, 444.
 Benetti S., Cappellaro E., Turatto M. et al. 1994, *A & A*, **285**, 147.
 Benetti S.; Cappellaro E.; Danziger I. J. et al. 1998, *MNRAS*, **294**, 448.
 Benetti S., Turatto M., Balberg S. et al. 2001, *MNRAS*, **322**, 361.
 Blanton E. L., Schmidt B. P., Kirshner R. P. et al. 1995, *AJ*, **110**, 2868.
 Buta, R. J. 1982, *PASP*, **94**, 578.
 Cardelli J. A., Clayton G. C., Mathis J. S. 1989, *ApJ*, **345**, 245.
 Castor J. I. 1970, *MNRAS*, **149**, 111.
 Catchpole R. M., Whitelock P. A., Feast M. W. et al. 1988, *MNRAS*, **231**, 75.
 Chugai N. N. 1994, *ApJ*, **428**, 17.
 Chugai N. N. and Danziger I. J. 2003, *AstL*, **29**, 649.
 Clocchiatti A. et al. 1996a, *AJ*, **111**, 1286.
 Clocchiatti A. et al. 1996b, *ApJ*, **462**, 462.
 Clocchiatti A.; Wheeler J. C.; Benetti S.; Frueh M. 1996c, *ApJ*, **459**, 547.
 Clocchiatti A.; Suntzeff N. B.; Phillips M. M.; Filippenko A. V.; Turatto M. et al. 2001, *ApJ*, **553**, 886.
 Danziger I. J.; Bouchet P.; Gouiffes C.; Lucy L. B. 1991, in “*Supernova 1987A and other supernovae*”, *ESO Conference and Workshop Proceedings*, Ed. by I. J. Danziger and Kurt Kjar, , 217.
 de Kool M., Li H. & McCray R. 1998, *ApJ*, **503**, 857.
 Elmhamdi A. et al. 2003a, *MNRAS*, **338**, 939.
 Elmhamdi A.; Chugai N. N.; Danziger I. J. 2003b, *A & A*, **404**, 1077.
 Elmhamdi A., Danziger I. J., Cappellaro E. et al. 2004, *A & A*, **426**, 963.
 Elmhamdi A.; Danziger I. J.; Branch D. et al. 2006, *A & A*, **450**, 305.
 Elmhamdi A. et al. 2011, *ApJ*, **731**, 129.
 Foley R. J.; Papenkova M. S.; Swift B. J. et al. 2003, *PASP*, **115**, 1220.
 Filippenko A. V., Porter A. C. & Sargent W. 1990, *AJ*, **100**, 1575.

- Filippenko A. V. 1997, *ARA & A*, **35**, 309.
- Fransson C.; Chevalier R. A. 1987, *ApJ*, **322**, 15.
- Fransson C.; Chevalier R. A. 1989, *ApJ*, **343**, 323.
- Fransson C.; Houck J.; Kozma C. 1996, in “*Supernovae and supernova remnants*”. *Proceedings of the IAU Colloquium 145*; Ed. by Richard McCray and Zhenru Wang, , 211.
- Fransson C.; Chevalier R. A.; Filippenko A. V. et al. 2002, *ApJ*, **572**, 350.
- Gomez G. & Lopez R. 2002, *AJ*, **123**, 328.
- Houck J. C. & Fransson C. 1996, *ApJ*, **456**, 811.
- Hamuy M., Pinto P. A., Maza J. et al. 2001, *ApJ*, **558**, 615.
- Hamuy M. 2003, *ApJ*, **582**, 905.
- Jeffery D. J. & Branch D. 1990, in “*Supernovae*”, *Sixth Jerusalem Winter School for Theoretical Physics (Singapore: World Scientific)*; Ed. by J.C. Wheeler, T. Piran, & S. Weinberg, , 149.
- Kirshner R. P. & Kwan J. 1975, *ApJ*, **197**, 412.
- Leibundgut B., Kirshner R. P., Pinto P. A. et al. 1991, *ApJ*, **372**, 531.
- Lewis J. R., Walton N. A., Meikle W. P. S. et al. 1994, *MNRAS*, **266**, 27.
- Li H. & McCray R. 1992, *ApJ*, **387**, 309.
- Lucy L. B.; Danziger I. J.; Gouiffes C.; Bouchet P. 1989, in “*Structure and Dynamics of the Interstellar Medium*”, *Proceedings of IAU Colloq. 120*. Ed. by Guillermo Tenorio-Tagle, Mariano Moles, and Jorge Melnick, , .
- Maeda K.; Nomoto K.; Mazzali P. A.; Deng J. 2006, *ApJ*, **640**, 854.
- Matheson T. et al. 2001, *AJ*, **121**, 1648.
- Maurer, J.I. et al. 2010, *MNRAS*, **402**, 161.
- Mazzali, P.A. et al. 2010, *MNRAS*, **408**, 87.
- McCray R. 1996, in “*Supernovae and supernova remnants*”. *Proceedings of the IAU Colloquium 145*; Ed. by Richard McCray and Zhenru Wang, , 223.
- Melendez J.; Barbuy B.; Spite F. 2001, *ApJ*, **556**, 858.
- Menzies J. W. 1991, in “*Supernova 1987A and other supernovae*”, *ESO Conference and Workshop Proceedings*, Ed. by I. J. Danziger and Kurt Kjar, , 209.
- Nomoto K. et al. 1984, *ApJ*, **286**, 644.
- Nomoto K.; Filippenko A. V.; Shigeyama T. 1990, *A & A*, **240**, 1.
- Nomoto K. et al. 1997, *Nucl. Phys.*, **616**, 79.
- Pastorello A.; Turatto M.; Benetti S.; Cappellaro E.; Danziger I. J. et al. 2002, *MNRAS*, **333**, 27.
- Pastorello A.; Aretxaga I.; Zampieri L.; Mucciarelli P.; Benetti S. 2002, *ASPC*, **342**, 285.
- Patat F., Cappellaro E., Danziger J. et al. 2001, *AJ*, **555**, 900.
- Popov D. V. 1993, *ApJ*, **414**, 712.
- Pozzo M.; Meikle W. P. S.; Rayner J. T et al. 2006, *MNRAS*, **368**, 1169.
- Qiu Y. et al. 1999, *AJ*, **117**, 736.
- Richardson D.; Branch D.; Baron E. 2006, *AJ*, **131**, 2233.
- Ruiz-Lapuente P., Canal R., Kidger M., Lopez R. et al. 1990, *ApJ*, **100**, 782.
- Sahu D. K.; Anupama G. C.; Srividya S.; Muneer S. 2006, *MNRAS*, **372**, 1315.
- Sauer D. N.; Mazzali P. A.; Deng J. et al. 2006, *MNRAS*, **369**, 1939.
- Schlegel E. M. & Kirshner R. P. 1989, *AJ*, **98**, 577.
- Schmidt B. P., Kirshner R. P., Schild R. et al. 1993, *ApJ*, **105**, 2236.
- Shigeyama T.; Nomoto K.; Tsujimoto T.; Hashimoto M. 1990, *ApJ*, **361**, 23.
- Sollerman J., Leibundgut B. & Spyromilio J. 1998, *A & A*, **337**, 207.
- Spyromilio J. & Pinto P. A. 1991, in “*Supernova 1987A and other supernovae*”, *ESO Conference and Workshop Proceedings*, Ed. by I. J. Danziger and Kurt Kjar, , 423.
- Suntzeff N. B. & Bouchet P. 1991, In “*Supernovae*”, Ed. Woosley S. E., Springer-Verlag, New York, , 12.
- Taubenberger, S. et al. 2009, *MNRAS*, **397**, 677.
- Thielemann F. K., Nomoto K. & Hashimoto M. 1996, *ApJ*, **460**, 408.
- Turatto M., Cappellaro E., Benetti S. & Danziger I. J. 1993, *MNRAS*, **265**, 471.

- Turatto M., Mazzali P. A., Young T. R. et al. 1998, *AJ*, **498**, 129.
Uomoto A. 1986, *ApJ*, **310**, 35.
Uomoto A. & Kirshner R. P. 1986, *ApJ*, **308**, 685.
VandenBerg D. A.; Swenson F. J.; Rogers F. J.; Iglesias C. A.; Alexander D. R. 2000, *ApJ*, **532**, 430.
Woosley S.E. & Weaver T.A. 1995, *ApJ*, **101**, 181.
Zampieri L. et al. 2003, *MNRAS*, **338**, 711.

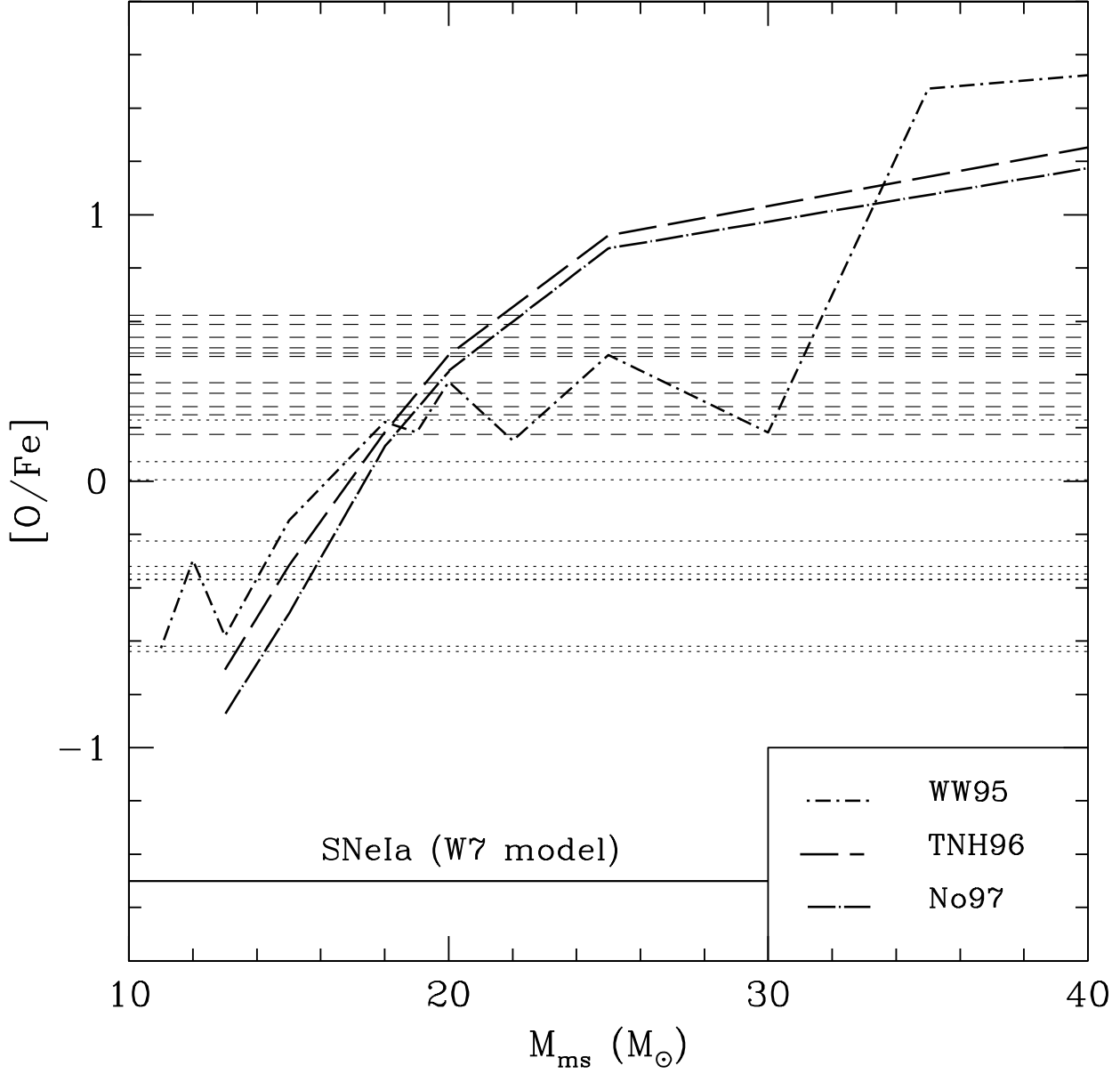


Fig. 6. The [O/Fe] yields ratio as a function of the initial mass according to the theoretical models of Woosley & Weaver 1995 (short dot-dashed line), Thielemann, Nomoto & Hashimoto 1996 (long dashed line) and Nomoto et al. 1997 (long dot-dashed line). For each event the corresponding estimated [O/Fe] value is plotted horizontally (SNe II with horizontal dashed lines, while horizontal dotted lines correspond to SNe Ib-c). Typical value for thermonuclear SNe is also reported for comparison (horizontal continuous line, Nomoto et al. 1984).

Table 1: Parameters data of the CCSNe sample

SN name	SN Type	Parent galaxy	Distance (Mpc)	A_V^{tot}	M_{Ni} M_{\odot}	M_{oxy} M_{\odot}	References
1987A	II	LMC	0.05	0.6	0.075	1.5 – 2	1, 2
1988A	IIP	NGC 4579	22.95	0.136	0.088	0.7 – 1.38	7, 8
1988H	IIP	NGC 5878	28.47	0.47	0.033	0.79 – 1.1	8
1990E	IIP	NGC 1035	16.18	1.2	0.043	0.94 – 1.3	10, 13
1991G	IIP	NGC 4088	14.11	0.065	0.021	0.36 – 0.49	9
1992H	IIP	NGC 5377	29.07	0.054	0.123	0.98 – 1.5	14
1995ad	IIP	NGC 2139	23.52	0.112	— — —	— — —	17
1997D	IIP	NGC 1536	16.84	0.07	0.0065	— — —	11, 12, 15
1999em	IIP	NGC 1637	8.8	0.31	0.027	0.3 – 0.54	3, 4, 5
2002hh	IIP	NGC 6946	5.9	3.3 & 1.7	0.07	0.78 – 1.05	18
2004et	IIP	NGC6946	5.6	1.27	0.06	0.75 – 1.8	19
1970G	IIL-P	NGC 5457	7.2	0.4	0.051	0.88 – 1.18	6, 16
1980K	IIL	NGC6946	5.6	1.5	0.046	0.57 – 0.76	35, 36
1990I	Ib	NGC4650	39.3	0.4	0.11	0.7 – 1.35	20
1996aq	Ib/c	NGC5584	24.32	0.124	— — —	0.4 – 1	17
1983I	Ic	NGC4051	22.08	0.043	0.15	0.43	21
1983N	Ib	NGC5236	4.46	0.51	0.15	0.43	21, 22
1990B	Ib/c	NGC4568	15.27	2.64	0.14	0.4	23, 24, 25
1984L	Ib	NGC991	23.44	0.32	0.37	0.58	25, 26
1985F	Ib	NGC4618	7.3	0.0	0.1	0.3	26
1987M	Ic	NGC 2715	22.7	1.3	0.26	0.4	27, 28
1994I	Ic	NGC 5194	8.32	0.93	0.07	0.22	29
1993J	IIf	M81	3.64	0.6	0.1 – 0.14	0.5	30, 31, 32
1996N	Ib	NGC 1398	22	0.0	— — —	0.1 – 0.3	30
1998bw	Ic	ESO 184-G82	35.16	0.2	0.4 – 0.5	5 – 6	33
2002ap	Ic	M74	7.9	0.24	0.09	0.6	34

REFERENCES:

1- Arnett 1996; 2- Hirata et al. 1987; 3- Baron et al. 2000; 4- Elmhamdi et al. 2003; 5- Hamuy et al. 2001; 6- Kirshner & Kwan 1975; 7- Ruiz-lapuente et al. 1990; 8- Turatto et al. 1993; 9- Blanton et al. 1995; 10- Benetti et al. 1994; 11- Turatto et al. 1998; 12- Benetti et al. 2001; 13- Schmidt et al. 1993; 14- Clocchiatti et al. 1996; 15- Zampieri et al. 2003; 16- Barbon et al. 1973; 17- Based only on the present work; 18- Pozzo et al. 2006; 19- sahu et al. 2006; 20- Elmhamdi et al. 2004; 21- Shigeyama et al. 1990; 22- Clocchiatti et al. 1996c; 23- Clocchiatti et al. 2001; 24- Gomez & Lopez 2002; 25- Richardson et al. 2006; 26- Schlegel & Kirshner 1989; 27- Filippenko et al. 1990; 28- Nomoto et al. 1990; 29- Sauer et al. 2006; 30- Sollerman et al. 1998; 31- Lewis et al. 1994; 32- Barbon et al. 1995; 33- Maeda et al. 2006; 34- Foley et al. 2003; 35- Buta 1982; 36- Uomoto & Kirshner 1986.

NOTE: the net effect from the uncertainty sources, see text, indicate a variation in the calculated oxygen masses within 15 – 30%. The estimated iron mass is found to be less biased, especially for type II events.